FIB line marking as a tool for local erosion/deposition/fuzz formation measurements in ASDEX Upgrade during the He campaign

M. Rasinski a*, S. Brezinsek a, A. Kreter a, T. Dittmar a, K. Krieger b, M. Balden b, P. de Marne b, R. Dux b, M. Faitsch b, A. Hakola c, J. Likonen c, E. Tsitrone d, V. Rohde b, ASDEX Upgrade Team 1, EUROfusion MST1 Team 2

a Forschungszentrum Jülich GmbH, Institut für Energie- und Klimaforschung – Plasmaphysik, 52425 Jülich, Germany

b Max-Planck-Institut für Plasmaphysik, 85748 Garching b. München, Germany

c VTT Technical Research Centre of Finland Ltd., P.O. Box 1000, FI-02044 Espoo, Finland

d CEA, Institute for Research on Fusion by Magnetic confinement, 13108 Saint-Paul-Lez-Durance, France

*Corresponding author e-mail: m.rasinski@fz-juelich.de

Highlights

Abstract

Tungsten (W) is the prime candidate for the plasma facing material in present and future fusion devices. When exposed to a plasma containing He ions, W can exhibit creation of sub-surface nano-bubbles leading to formation of nano-tendrils called fuzz. Formation of W fuzz was confirmed by many laboratory experiments including He loading in linear plasma devices. There is, however, limited experience related to the parameter space for fuzz formation and re-erosion in a tokamak environment. For this reason a dedicated experiment was carried out in ASDEX Upgrade (AUG) during its 2022 He campaign to study the evolution of fuzz-like W structures.

Twelve tungsten samples were mechanically polished to a mirror-like surface finish. Six of them were subsequently exposed to a He plasma in the PSI-2 linear device in order to establish a fuzz layer with a thickness of 600 – 800 nm. Before exposure in AUG, all samples were pre-characterized by Focused Ion Beam (FIB) cross-sectioning. In total 48 FIB cross-sections with line markings for quantification of local erosion, deposition and fuzz formation were prepared – 4 on

each sample. The samples were placed in two parallel poloidal rows spanning a range of 20 cm around the outer strike line position (OSP). They were subsequently exposed in AUG to a series of 14 consecutive discharges, 8 in H-mode and 6 in L-mode.

Detailed analysis by means of electron microscopy revealed on the samples regions of erosion, deposition and fuzz formation. Below the H-mode OSP, homogeneous co-deposits containing W and O, with a thickness up to 400 nm, were found. In the close vicinity of the H-mode OSP, significant erosion of pre-exposure PSI-2 fuzz was observed. The erosion reached up to 100 – 250 nm, depending on the location. In addition, the initially polished samples did not show any newly formed fuzz in that zone. Above the H-mode OSP, new fuzz was formed with a thickness of up to 800 nm. There was no Mo found in the newly formed fuzz. Pre-exposure PSI-2 fuzz was either removed or modified.

1. Introduction

Tungsten (W) is characterised by a high melting point and high thermal conductivity and correspondingly a high resistance to thermal and particle fluxes. W has also relatively low sputtering yield as well as low retention of hydrogen isotopes [1]. For that reasons W is employed in current fusion devices as JET [2], ASDEX Upgrade (AUG) [3] or WEST [4] as a divertor and first wall plasma facing material (PFM). In future fusion devices such as ITER [5] or DEMO [6] it is also foreseen to use W as PFM, especially in the divertor region.

When exposed to a plasma containing He ions, on the surface of W hair-like structures called "fuzz" can be formed. The full mechanism of fuzz formation is not yet completely understood, but it is considered to involve several processes, including creation of nano-bubbles and their coalescence beneath the surface [7]. Summary of a current state of fuzz growth understanding can be found elsewhere [8]. Fuzz formed on the surface of W exhibits different properties with respect to erosion, thermal conductivity or H isotopes retention. For that reason it is very important to know its properties as well as fuzz formation conditions under given operation conditions of a fusion device.

The formation of tungsten fuzz was widely studied in many linear plasma devices [9][10][11][12][13], which lead to a general description of conditions required for fuzz formation. Essential parameters for fuzz formation are: (i) He ion flux greater than 2 x 10^{24} ions/m^2 (also for the He fraction in a mixed plasma exposure), (ii) He ion energy greater than 20 eV and (iii) W

surface temperature (T_{surf}) in the range 1000 to 2000 K [10]. It is also known that the presence of molybdenum (Mo) may affect the W fuzz formation conditions, namely by reducing the required $T_{surf.}$ [14]. For that reason it is important to avoid Mo contamination when investigating the W fuzz evolution.

Despite a vast amount of experimental results from linear plasma devices, there is still limited experience on W fuzz formation in fusion devices. There have been attempts to study the growth of fuzz in tokamaks and stellerators such as Alcator C-Mod [15], AUG [16][17], LHD [18], WEST [19] or JET. Up to now no pure W fuzz was obtained for several of reasons. Alcator C-Mod was equipped with plasma facing components made of both Mo and W so that the created fuzz was an admixture of W and Mo [15]. A similar issue arose in an experiment during the AUG He campaign in 2019. A set of W samples was mounted in a dedicated target tile made of Titanium-Zirkonium-Molybdenum (TZM) alloy for exposure with the divertor manipulator. As a consequence, the grown fuzz contained up to 20 at. % of Mo [20]. During the WEST dedicated He campaign, no W fuzz-like structures were observed, although the main criteria for W fuzz formation were fulfilled [19]. These examples clearly show that the conditions for W fuzz formation in a tokamak are much more complex than in a linear devices. Criteria like W erosion and re-deposition as well as fuzz annealing are expected to play a significant role, and cannot be studied in linear devices.

In view of previous experiments the attempt to study W fuzz in fusion devices under well-defined conditions is important, particularly aiming at a reduced presence of impurity species. This paper presents results from AUG during the He campaign 2022 where for the first time formation of pure W fuzz layers (without any Mo contamination) could be studied.

2. Experimental

A set of twelve W samples with a size of $33 \times 12 \times 5$ mm^3 were mechanically polished to obtain a mirror like surface finish. Six of them were subsequently exposed to He plasma discharges in the PSI-2 linear device. Details of the experimental setup of PSI-2 are described in [21]. A bias voltage of -100 V was applied to the samples, resulting in an incident ion energy in the range of 60 - 80 eV. The incident ion flux was in the range of 8.4×10^{21} m^{-2}s^{-1} and the incident ion fluence was 1.5×10^{25} m^{-2}. Ion flux and energy were measured by a Langmuir probe. The surface temperature, T_{surf},

during plasma exposure was in the range 1150 – 1200 K. In the following, the samples with W fuzz created in PSI-2 will be named "pre-damaged".

The surface morphology of the samples before and after plasma exposure was analysed using a field emission scanning electron microscope (FE-SEM) [Zeiss Crossbeam 540]. A dual beam scanning electron microscope/focused ion beam (SEM/FIB) device, equipped with an energy dispersive X-ray analyser (EDX) was used for both surface imaging, cross section preparation, TEM lamella preparation, cross section imaging and elemental composition analysis. For each sample four FIB cross-sections were prepared, two in the centre and two in a corner of each sample. Each cross-section was rotated in a way that the analysed side of a cross-section was facing in a different direction. Moreover, on each cross-section, additional line markings were created using a 10pA FIB beam. The line markings, consisting of five lines spaced every 1 μm, served as a distinct reference for local erosion and re-deposition measurements. In particular cases, when the line marking system was covered by co-deposition, additional gentle cleaning with a 50pA Ga beam was used to make the marker visible again.

The pre-characterised samples were subsequently mounted as inserts in two dedicated tungsten target tiles for exposure with the AUG DIvertor Manipulator (DIM-II) [22]. **Figure 1** shows the poloidal cross-section of AUG with the two plasma equilibria and the geometries of both the manipulator probe head and local diagnostics used in the experiment. The samples were installed in the tiles in two vertical rows, with the pre-damaged samples in one row and the polished samples in the adjacent row. **Figure 2** (c) shows a photo of the tile with installed samples before AUG He exposure and (b) a photo of the retrieved tile after AUG He exposure.

The samples were exposed in two regimes of local plasma conditions, by executing two series of L-mode and H-mode discharges, respectively. The two scenarios were spatially separated on the tile by adjusting the outer strike point location (OSP) between the two discharge series as shown in **Fig. 1**. Apart from the OSP position, both scenarios were executed in the same magnetic configuration at identical plasma current (I_p = 0.8 MA) and toroidal magnetic field (B_t = -2.5 T). The H-mode discharges were heated with neutral beam injection (NBI, P_{NBI} = 6 MW) and central Electron Cyclotron Resonance Heating (ECRH, P_{ECRH} = 4 MW). For the L-mode discharges the heating power was reduced to P_{ECRH} = 1 MW without NBI heating.

The local distribution of the integrated OSP residence time across the tile is shown in **Figure 2a**. In the first eight discharges the H-mode plasma scenario was used with the OSP located on the third sample counted from the bottom of the tile. Due to an instability in the plasma control system,

the OSP oscillated over the sample in a range of ≈20mm. The total ion fluence near OSP in the H-mode discharge series derived from Langmuir probe measurements reached values of 3.4×10^{24} m^{-2} assuming He^{2+} as dominant plasma ion species. Further away from the OSP (sample positions 4 and 5) the ion fluence was falling off to ≈2×10^{24} m^{-2}. In the subsequent five discharges the L-mode scenario was used with the OSP moved down to the middle of the lowest samples. Near OSP the total ion fluence in these discharges was a factor 10 smaller at ≈0.3×10^{24} m^{-2}.

During the H-mode discharges the local surface temperature of the samples was measured by analysis of their IR emission, which was recorded by a thermography camera viewing the two tiles exposed with the divertor manipulator through an image guide optics at the central column (see **Figure 1**). Because of the glass fibres used for image transmission, the observation was limited to the Short Wavelength Infra Red (SWIR) spectral range around 1.7um. The camera system was calibrated directly after the campaign by a calibrated tungsten filament lamp installed at the manipulator tile position. The derived time evolution of the apparent surface temperature (assuming a tungsten emissivity of ε=0.1) at the centre and edges of the samples is shown in **Figure 7**. Unfortunately, adaptive exposure time control was not yet implemented in the camera acquisition software so that in the hottest areas the camera saturated at an apparent surface temperature of 1800 K, with actual temperatures estimated to reach values above 2500 K near OSP.

3. Results and discussion

The visual changes induced by the plasma exposure of the samples are illustrated by **Figure 2**, which shows the tungsten tile with installed samples before (c) and after (b) AUG He plasma exposure. Already this initial impression suggests significant modification of the surface morphology by the incident He ion particle and power load. Based on the observed surface evolution and the cross-section morphology changes, the position of the samples across the tile can be divided into 5 regions , namely (i) below the L-mode OSP, (ii) near the L-mode OSP, (iii) in-between L-mode and H-mode OSPs, (iv) near the H-mode OSP and (v) above the H-mode OSP. Each region is characterised by a different surface modification pattern resulting from the corresponding variation of He plasma-surface interaction.

(i)   Below the L-mode OSP

Below the L-mode OSP, near the lower edge of the tile, the surface morphology of both polished and pre-damages samples remains untouched. Structure and thickness of the pre-damage W-fuzz are preserved with no visible damage. The surface of the polished sample shows no indication of

He induced damage. FIB prepared cross-sections also show no sign of erosion or re-deposition. Moreover, the prepared FIB line markings on both cross-sections (pre-damaged and polished) confirm that neither erosion nor co-deposition occurred at this location.

(ii)   Near the L-mode OSP

The surface of the samples close to the L-mode OSP is visibly smoothened. FIB prepared cross-sections reveal local erosion. The top part of the pre-damage fuzz is removed, but the near-surface regions remains untouched. It is, however difficult to measure exactly the eroded amount of the fuzz structure because of its inhomogeneity. The measured local erosion on the polished surface was in the range of 50 nm at most for an accumulated He^{2+} fluence from the L-mode discharges of $\approx 0.3 \times 10^{24}$ m^{-2}.

(iii)   In-between L-mode and H-mode OSP

The region in-between the two OSP locations is characterized by visible smoothening of the sample surface after exposure. Pre-damage fuzz is completely covered by deposited material. FIB cross-sections confirm the existence of a co-deposition layer containing W and O, with thickness varying depending on the location on the tile. **Figure 3** shows SEM images of the cross-section before (a, c) and after (b, d) AUG plasma exposure in the location where the thickness of co-deposited layer is the largest. Green lines indicate the region where the co-deposited layer was formed. The thickness reached 100 nm and 250 nm for polished and pre-damaged sample, respectively. Below the co-deposition layer, pre-damaged fuzz shows no significant modifications. The structure of the co-deposited layer is porous, as illustrated in **Figure 4**. The figure shows the STEM image of the pre-damaged sample with the co-deposited layer after exposure. The structure of pre-damage fuzz tendrils is porous, containing He nano-bubbles. The red line indicated the position of EDX line scan for chemical analysis together with given intensity profiles of W, O and Mo along the line. Apart from W, the deposited layer contains at most 40 at. % of O. No trace of Mo was found. The porous structure of deposits formed during AUG discharges is very similar to those previously reported [23].

(iv)   Near the H-mode OSP

Figure 5 presents SEM images of the FIB prepared cross-sections before (a, c) and after (b, d) AUG plasma exposure. The top surface of the pre-damaged fuzz is collapsed whereas the polished sample reveals a typical erosion pattern. The bottom part of the pre-damage fuzz is preserved, as its inner structure looks the same before and after AUG plasma exposure. Green lines indicate the erosion rate which was calculated based on the FIB line markings. The local erosion reached 150

– 250 nm depending on the substrates grain orientation. Different grains exhibited different erosion rate. The accumulated fluence in the complete L-mode and H-mode discharge series near the H-mode OSP reached 3.4 x 10^{24} m^{-2}.

(v)   Above the H-mode OSP

In the region above the H-mode OSP new formation of new W-fuzz was observed. The created fuzz is neither uniform nor homogenous on both polished and pre-damages samples. Pre-damaged fuzz from PSI-2 is removed and partly converted into new W-fuzz. **Figure 6** presents SEM images of the surface of samples exposed above the H-mode OSP. The bottom row shows pre-damaged samples and the top row the adjacent polished samples. Different fuzz structures, depending on the position on the tile are visible for both polished and pre-damaged samples. With decreasing distance to the OSP the fuzz tendrils appear coarser. Positions further away from the OSP shows formation of finer fuzz structures. Moreover, He bubble formation can be seen in-between the fuzz tendrils.

Since the accumulated fluence above the H-mode OSP is only slowly falling off from 3 x 10^{24} m^{-2} to 2 x 10^{24} m^{-2}, the differences in the morphology of the new W fuzz can be rather attributed to the locally varying surface temperature during the discharge. **Figure 7** presents apparent surface temperatures during single H-mode shot number 41473 with temperature values derived from SWIR camera IR intensities. The temperature evolution is shown at both pre-damaged (a) and polished (b) samples for different positions on the tile, as indicated with colored numbers. The color of the numbers at a given position corresponds to the color of the temperature time trace in the graphs. Formation of new W fuzz was observed at positions 1-4, with 5 being the location of the OSP. As discussed above, the camera measurement sutured for temperatures >1800 K. Local camera saturation occurred at position 3, and 4 for pre-damaged samples and at location 4 for polished samples. For similar values of T_{surf} (for example 3 polished and 2 pre-damaged – around 1500 K) a similar structure of the formed fuzz is observed. The same is seen for position 1 polished (top row) and 2 pre-damaged (bottom row), where the measured temperature was 1400 K and 1250 K, respectively. This demonstrates a very clear dependency of the structure of formed fuzz from T_{surf}. The lowest measured temperature at position 1 for polished samples was around 1000 K just above the sensitivity threshold of the camera. There, local fuzz formation with tendril thickness below 40 nm and height below 200 nm was observed.

Figure 9 shows SEM images of FIB-prepared cross-sections above the H-mode OSP where new fuzz was formed. T_{surf} at this position was saturated at the camera above 1800 K (position 4

on the top row of polished samples). The presented orientation of cross-sections was as they were machined on the samples. Red arrows indicate the direction of the incident He plasma flux. The SEM analysis shows here local fuzz formation inside the FIB trenches with the position where the fuzz is formed inside each trench clearly corresponding to the plasma direction.

4. Conclusions

Polished and pre-damaged (in the linear plasma device PSI-2) samples were exposed to subsequent series of identical H-mode and L-mode He plasma discharges in AUG. Each sample contained four FIB-prepared cross-sections with additional line markings for detailed, local measurement of erosion/deposition and fuzz formation and evolution. Below the OSP of the L-mode discharges no visible surface modification occurred. Near the OSP locations, in both L-mode and H-mode, local erosion was found. In-between the two OSP locations, deposited layers consisting of W and O and with a thickness up to 250 nm were observed. Above the H-mode OSP location, formation of new W fuzz was observed on both pre-damaged and polished samples. Fuzz formation was very non-uniform and strongly dependent on surface temperature. The fuzz thickness reached values of up to 1 μm and the single tendril thickness varied depending from the location on the sample and hence T_{surf}. With decreasing distance to the H-mode OSP, T_{surf} increased and by that thicker W fuzz tendrils were formed. No trace of Mo in the newly created W fuzz was observed, demonstrating that for the first time formation of Mo free W fuzz could be studied under tokamak He plasma exposure conditions.

References

[1] Pintsuk G 2012 Tungsten as a plasma-facing material Reference Module in Comprehensive Nuclear Materials (Amsterdam: Elsevier) vol 4 pp 551–81

[2] V. Philipps et al. / Fusion Engineering and Design 85 (2010) 1581–1586

[3] R. Neu et al. / Journal of Nuclear Materials 438 (2013) S34–S41

[4] J. Bucalossi et al Nucl. Fusion 62 (2022) 042007

[5] R.A. Pitts et al. / Journal of Nuclear Materials 438 (2013) S48–S56

[6] J.H. You et al. Nuclear Materials and Energy 16 (2018) 1–11

[7] S. Kajita, Journalof Nuclear Materials, vol. 418, no. 1-3, pp. 152–158, 2011.

[8] Wright, J.A.R., Tungsten 4, 184–193 (2022)

[9] Baldwin M. et al. 2008 Nucl. Fusion 48 035001
[10]   S Möller et al, Phys. Scr. T170 (2017) 014017
[11]   S. Kajita et al Nucl. Fusion 49 (2009) 095005

[12]   S. Kajita et al, J. Nucl. Mater., 548 (2021), Article 152844

[13]   T.J. Petty et al 2015 Nucl. Fusion 55 093033

[14]   M I Patino et al, Phys. Scr. T171 (2020) 014070

[15]   G.M. Wright et al, Nucl. Fusion 52 (2012) 042003

[16]   S. Brezinsek et al. / Nuclear Materials and Energy 12 (2017) 575–581

[17]   A. Hakola et al Nucl. Fusion 57 (2017) 066015

[18]   M. Tokitani et al. / Nuclear Materials and Energy 12 (2017) 1358–1362

[19]   E. Tsitrone et al Nucl. Fusion 62 (2022) 076028

[20]   M. Balden et al, Microscopy study of the growth and erosion of fuzz on tungsten
     by helium plasma exposure on ASDEX Upgrade, 24th International Conference on
     Plasma Surface Interactions in Controlled Fusion Devices (PSI 2020), virtuell, virtuell, 25
     Jan 2021 - 29 Jan 2021

[21]   A. Kreter. et al Fusion Sci. Technol. 68 (2015) 8

[22]   A. Hermann, et al.Fus. Eng. Design, 98 (2015), p. 1496

[23]   M. Rasinski et al. / Fusion Engineering and Design 86 (2011) 1753–1756

Figures and Tables
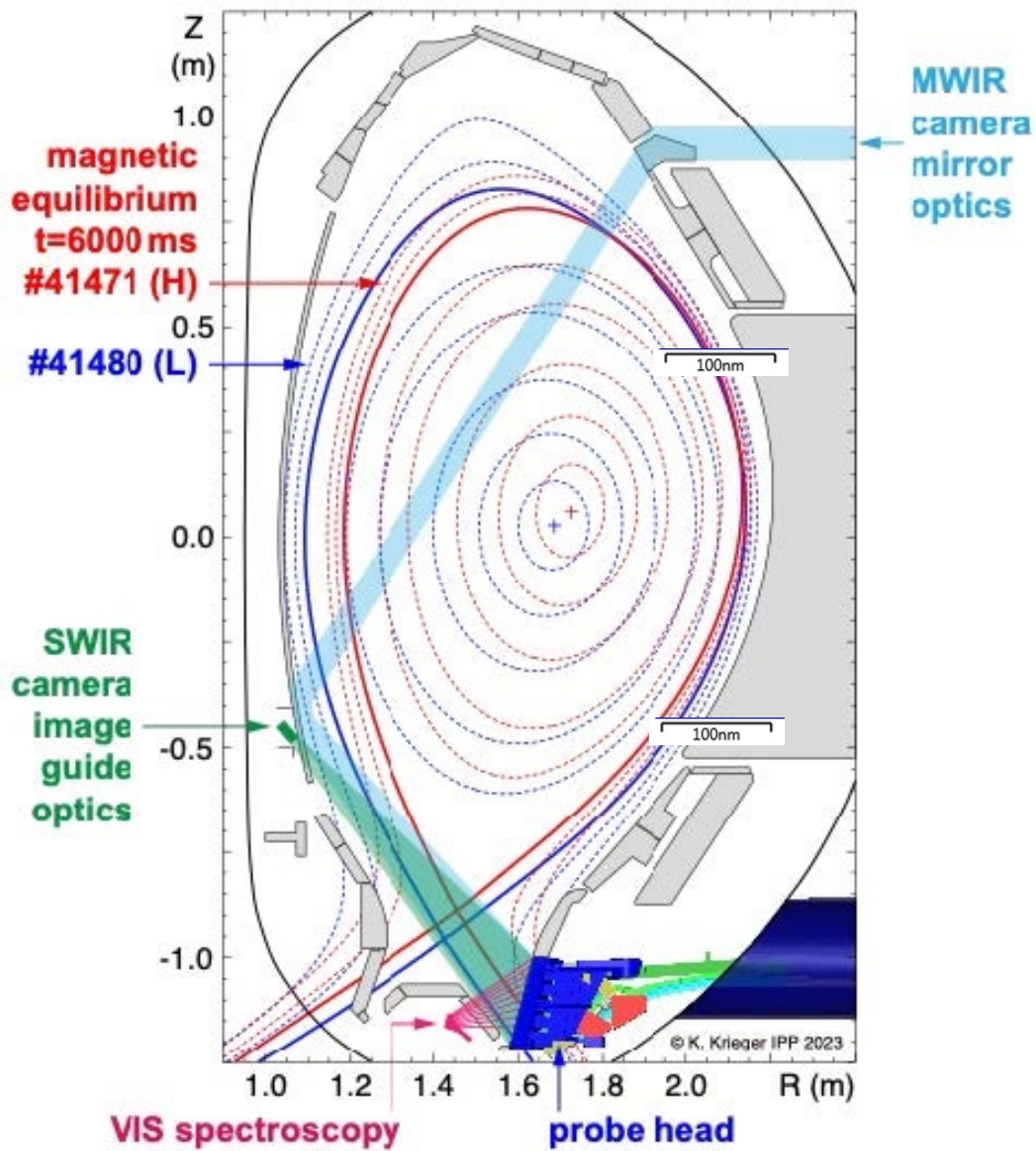
Figure 1 Poloidal cross-section of ASDEX Upgrade with marked divertor manipulator for samples exposure (probe head). Additionally magnetic equilibrium for H-mode and L-mode discharge are indicated.
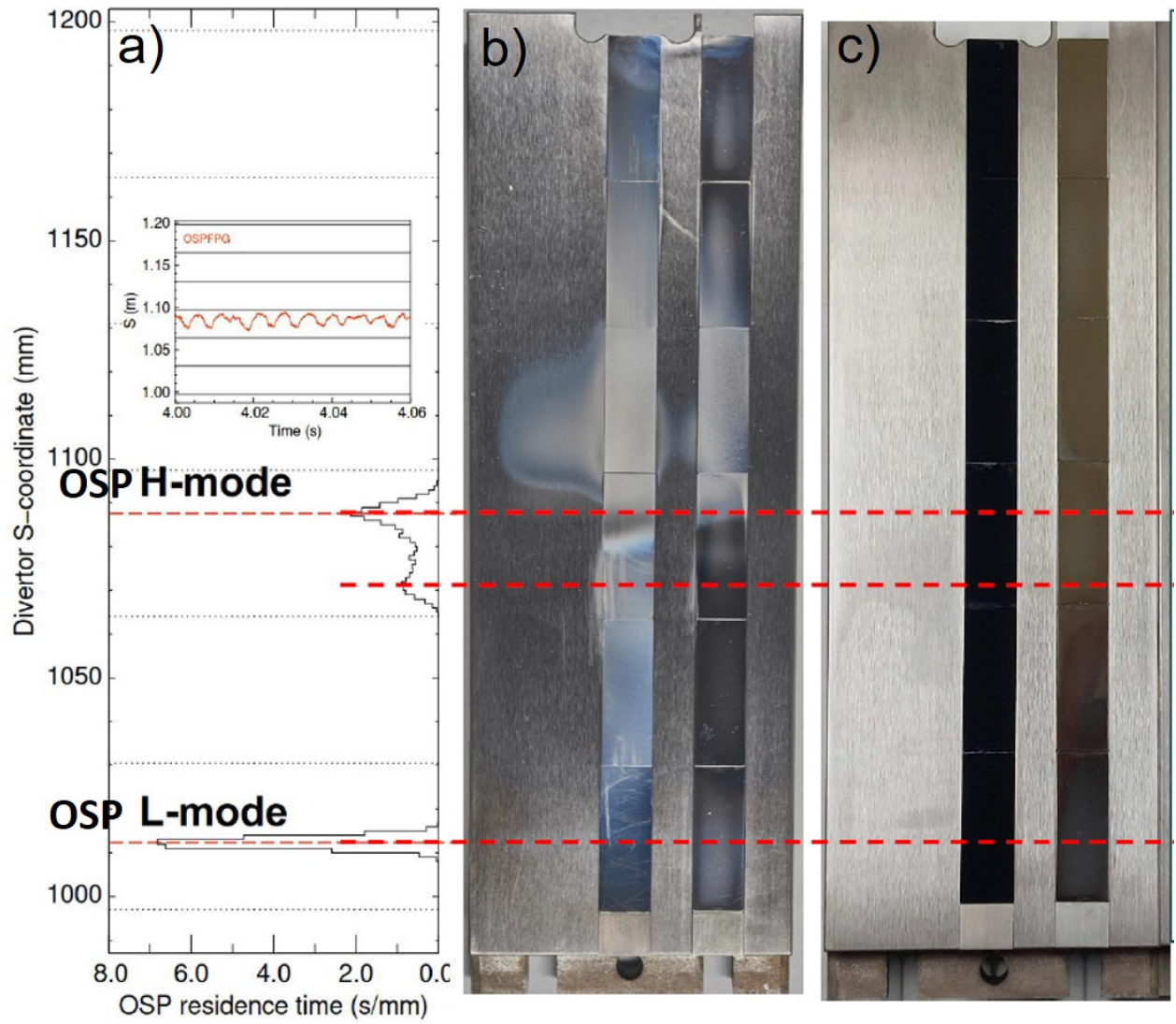
Figure 2 Images of divertor manipulator with installed samples before (c) and after (b) AUG He plasma exposure. Diagram (a) illustrates the divertor S-coordinate system including the position of L-mode and H-mode outer strike-line position (OSP).
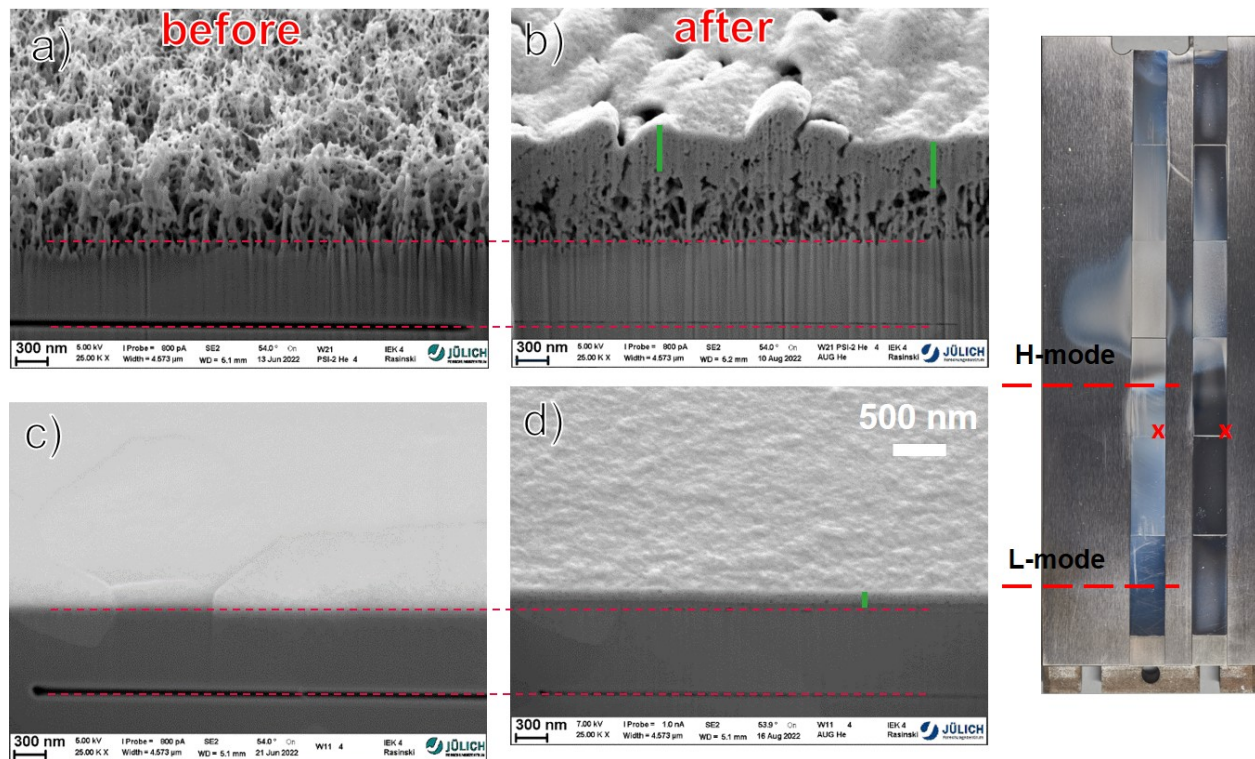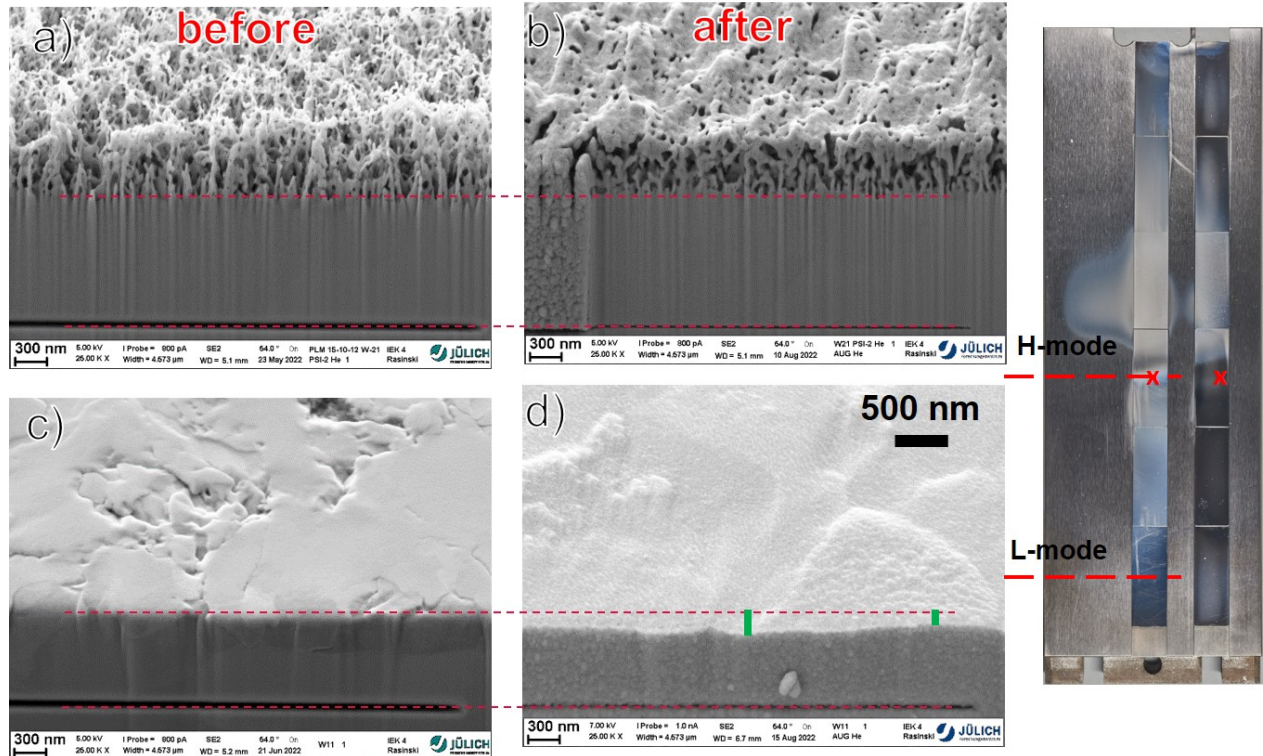
Figure 3 SEM images of FIB prepared cross-section with line marking before (a, c) and after (b, d) AUG He plasma exposure. Red x indicate to position on the sample were the image is coming from.
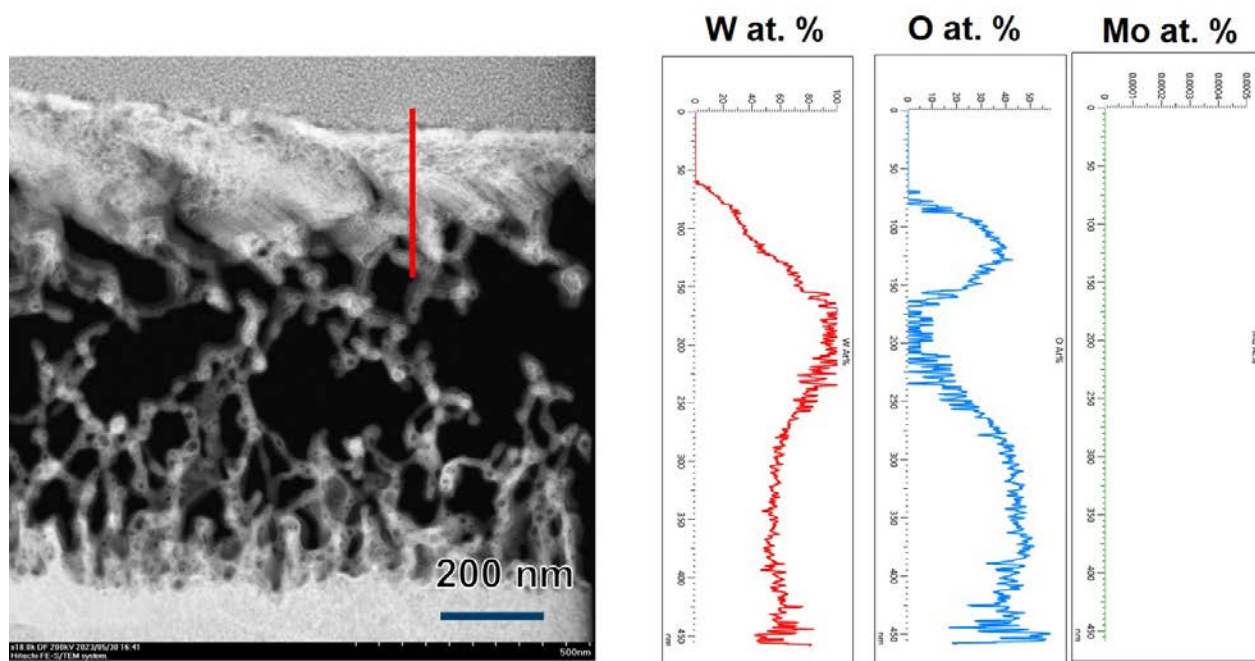
Figure 4 STEM image of PSI-2 pre-damaged sample after AUG He plasma exposure. Sample was placed inbetween H-mode and L-mode OSP where highest re-deposition rate was observed. EDX line scan across marked red line are attached illustrating distribution of W, O and Mo in at. %. Material above the surface is the Pt deposition layer coming from FIB thin lamella preparation.
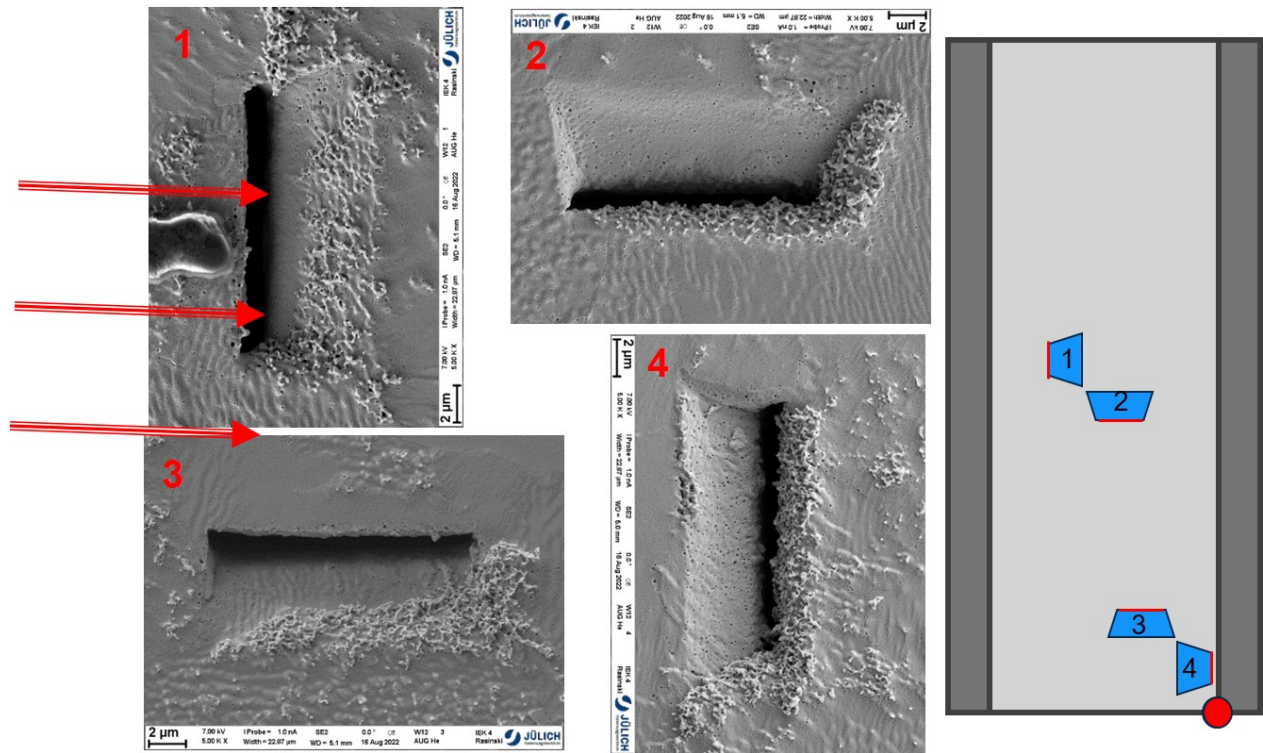

Figure 5 SEM images of FIB prepared cross-section with line marking before (a, c) and after (b, d) AUG He plasma exposure. Red x indicate to position on the sample were the image is coming from.
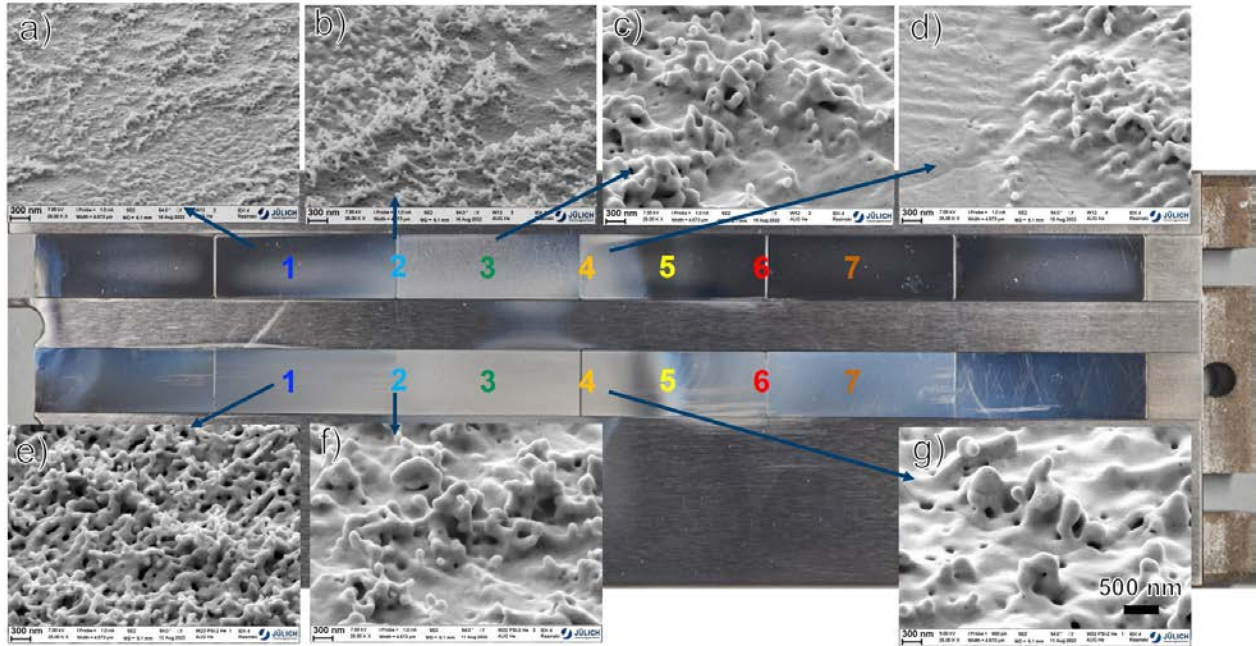
Figure 6 SEM surface images of polished (a-d) and pre-damaged (e-g) samples after AUG He plasma exposure. Different structure of formed W fuzz depending on the exposure position is illustrated.
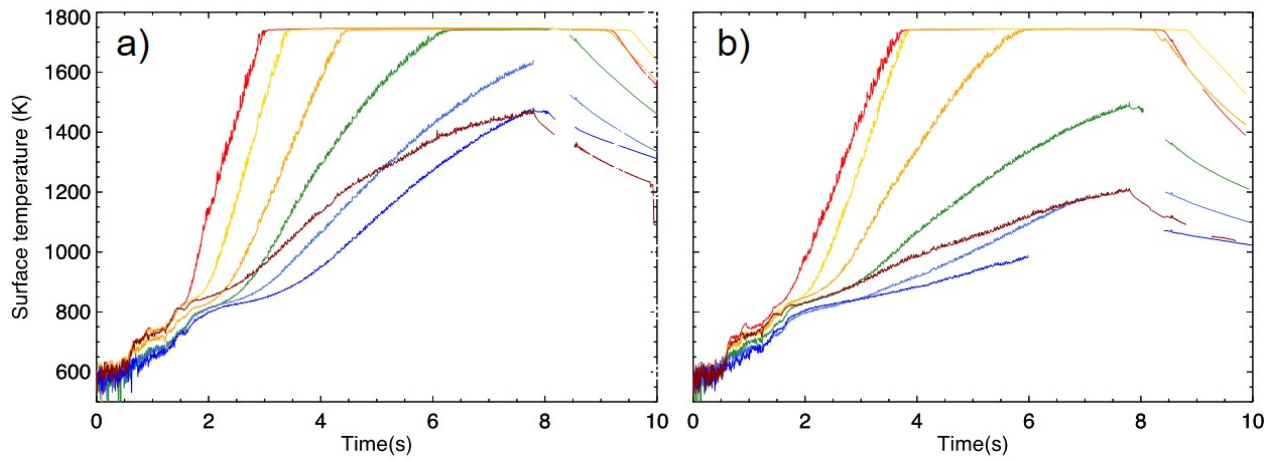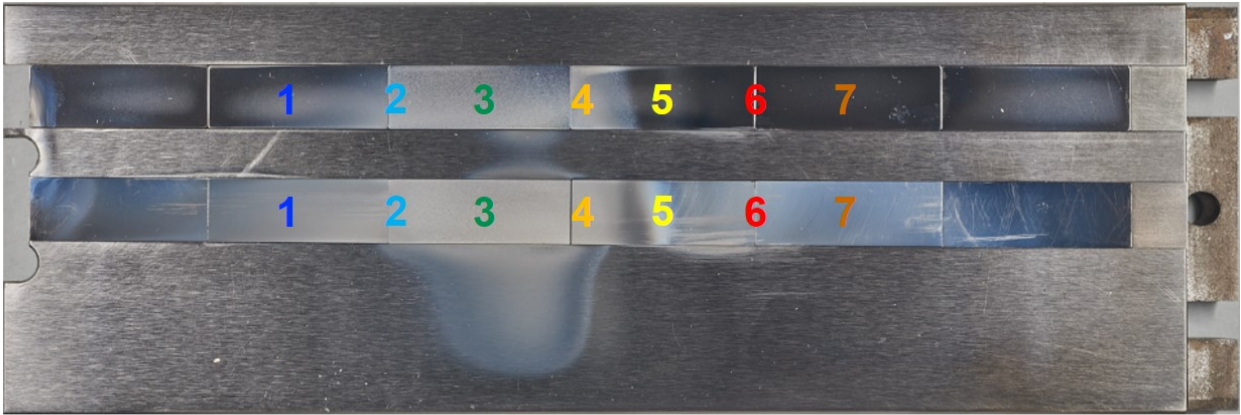
Figure 7 Apparent surface temperature during H-mode 41473 for a) pre-damaged and b) polished set of samples based on SWIR camera. Positions where the measurements are coming from are indicated with colour numbering corresponding to the colours on the temperature graph.

Figure 8 SEM images of the FIB prepared cross-sections oriented as they were cut on the sample. Sample was exposed above the H-mode OSP where new W fuzz was formed. Red arrows indicated the direction of the plasma. W fuzz formation inside the FIB trenches corresponding to plasma direction is visible.